ACS Photonics

Article

pubs.acs.org/journal/apchd5

Surface-Wave-Assisted Beaming of Light Radiation from Localized Sources

Angelo Angelini,*[,†,‡] Peter Munzert,[§] Emanuele Enrico,[‡] Natascia De Leo,[‡] Luciano Scaltrito,[†] Luca Boarino,[‡] Fabrizio Giorgis,[†] and Emiliano Descrovi*[,†]

[†]Dipartimento di Scienza Applicata e Tecnologia (DISAT), Politecnico di Torino, C.so Duca degli Abruzzi 24, I-10129, Torino, Italy

[‡]Nanofacility Piemonte, Istituto Nazionale di Ricerca Metrologica (INRIM), Strada delle Cacce 91, I-10135 Torino, Italy

[§]Fraunhofer Institute for Applied Optics and Precision Engineering IOF, Albert-Einstein-Strasse 7, D-07745 Jena, Germany

ABSTRACT: In analogy to the well-known plasmonic bull's eye, we introduce here an all-dielectric mutilayered ring structure with high-directivity antenna capabilities. Radiated energy from organic emitters localized within the ring center is resonantly transferred to surface modes on the multilayer and then diffracted in the free space. The structure can be obtained by properly applying the Bragg law to a diffraction pattern defined in the Fourier plane as a superposition of "caustics". This approach allows designing diffractive structures producing a surface-mode-assisted beaming of radiation out of the sample with an arbitrary propagation angle in two dimensions. Specifically, we demonstrate that an anisotropically periodic ring structure can beam fluorescence emission with a tilt angle of 11.5 deg from the normal direction. The proposed use of surface modes for manipulating light at a subwavelength scale can represent an interesting alternative to the more conventional all-plasmonic approach.

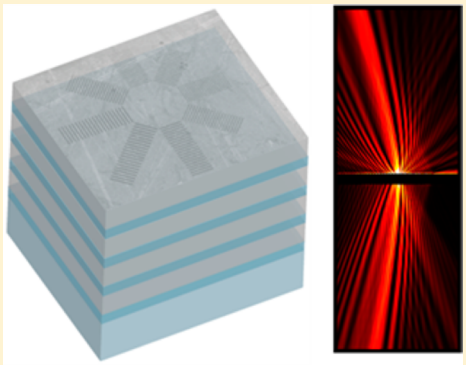

KEYWORDS: *directional emission, surface waves, photonic crystals, diffraction gratings*

In many applications such as optical sensing or lighting wherein ensembles of emitters randomly oriented radiate light almost isotropically, it may be desirable to take advantage of a suitably designed emission directivity.[1] It is well known that the modification of the photonic environment surrounding an emitter allows the tailoring of some of its emission properties, such as the quantum yield or the angular radiative pattern.[2] For example, when an emitting source is embedded into a transparent medium sustaining leaky guided modes, the radiated light can couple therein and finally leak into the substrate. In order to access this radiation, an approach based on leakage radiation collection can be employed.[3] Alternatively, photonic crystal-based structures characterized by a diffractive pattern allow the direct coupling of guided modes with free-space radiation in specific directions,[4,5] in such a way that collection optics operating in air can be used. In addition to guided modes, surface modes on corrugated photonic crystal interfaces have been demonstrated to drive a low-divergence beaming of light transmitted through small apertures.[6,7] Unfortunately, many of the conventional photonic crystal arrangements possess a surface structuration that intimately connects the propagation characteristics of the supported modes with the directions of the out-coupled radiation in the free space.[4] This feature limits the possibility of manipulating photonic crystal modes by means of further additional diffractive elements that should coexist on the crystal surface pattern.

An alternative to photonic crystals is represented by metallic structures supporting surface plasmons. On one hand, isolated or clustered metallic nanoparticles provide both a strong confinement of electromagnetic fields in subwavelength volumes and a control of the angular distribution of scattered radiation thanks to nanoantenna effects.[8−12] On the other hand, surface plasmons have been successfully used as local carriers of energy in combination with diffractive structures to shape the radiation pattern of dipolar emitters such as quantum dots, fluorophores, single-photon emitters,[13−16] and nanoscatterers such as single slits or holes in thin metallic films.[17−20] The main drawback of the fully plasmonic approach relies on the absorption losses in the plasmon-mediated energy transfer.

In a previous work we demonstrated the use of TE-polarized surface modes (referred to as Bloch surface waves, BSWs) on one-dimensional photonic crystals (1DPC) to beam radiative energy from localized sources to free-space radiation.[21] Here we introduce an anisotropic pattern on a 1DPC surface to beam fluorescence out of the structure at an arbitrary direction. In a recent paper, Zhan et al. used a plasmonic spiral antenna for obtaining an off-normal beaming of the fluorescence excited out of the center of symmetry of the structure.[22] In the present case, however, no plasmons are involved in the beaming mechanism since the structure is all-dielectric. Thanks to a design approach based on caustics curves in the Fourier plane, we managed to obtain and fabricate a quasi-concentric, locally periodic circular grating diffracting BSW-coupled fluorescence

Received: March 26, 2014
Published: June 18, 2014

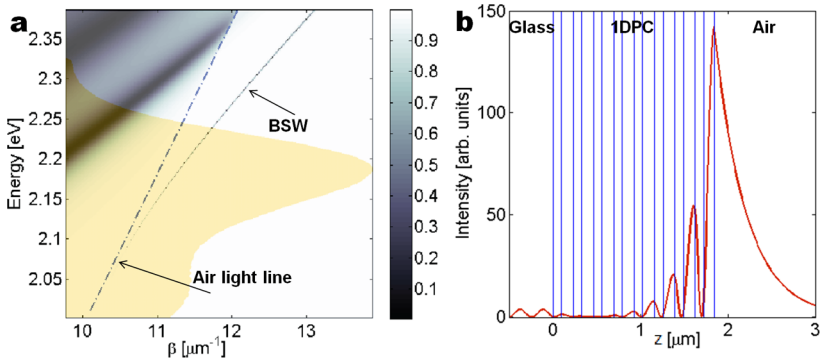

Figure 1. (a) Calculated reflectance map (TE polarization) for a 1DPC on glass as illuminated by plane waves with given energy $\hbar\omega$ and transverse wavevector $\beta = \omega c^{-1} n_s \sin\theta$, where θ is the incidence angle from the glass side and $n_s = 1.5$ is the refractive index of the glass substrate. The yellow-shaded region indicates the emission spectrum of the AlexaFluor 546 dye. (b) Cross-sectional view of the 1DPC and the corresponding transversal distribution of a TE-polarized BSW intensity at wavelength $\lambda = 570$ nm.

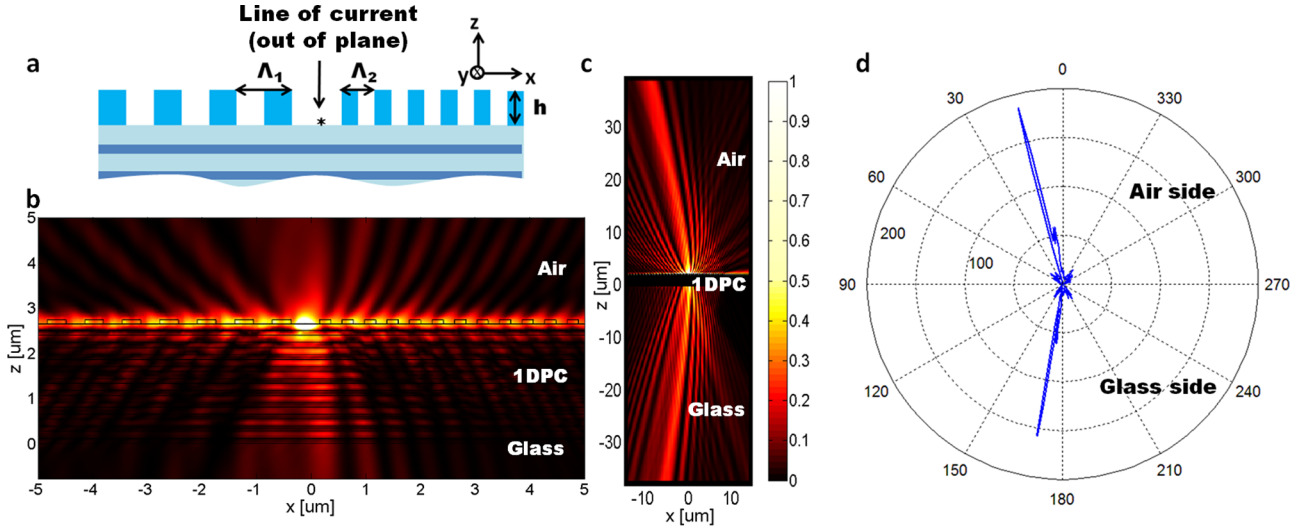

Figure 2. (a) Schematic view of the surface grating with a pair of linear gratings having height $h = 80$ nm and spatial period $\Lambda_1 = 670$ nm and $\Lambda_2 = 415$ nm, respectively. An emitting source as a line of current is located on a flat area sandwiched between the two gratings, oriented normally to the cross-section plane, along the y direction. (b) Calculated intensity distribution of the electromagnetic field ($\lambda = 570$ nm) emitted by the source. (c) The same as in (b) over a wider spatial range. (d) Calculated far-field radiation pattern.

at an arbitrary angle from the surface normal. Such a circular grating is anisotropic, as it shows a spatial periodicity varying with an azimuthal dependency.

A planar 1DPC employed in this work is constituted by a dielectric multilayer grown on a planar glass slice, as detailed in the Methods section. Such a periodic structure is designed to support TE-polarized BSWs in the visible range. The BSW is characterized by a dispersion curve that can be appreciated in Figure 1a, where a calculated TE-polarized reflectivity map is shown. Reflectivity values are calculated for a radiation with energy $\hbar\omega$ and a transverse wavevector component $\beta = \omega c^{-1} n_s \sin\theta$, where θ is the incidence angle from the glass side and $n_s = 1.5$ is the refractive index of the glass substrate. BSW at different energies correspond to β values associated with a dip in reflectivity. In Figure 1b a cross-sectional view of the BSW intensity ($\lambda = 570$ nm) calculated through the 1DPC is shown. The rather strong confinement of the BSW occurring close to the 1DPC surface promotes the near-field transfer of energy from emitting sources located on the 1DPC surface. In fact, it has been shown that an effect similar to the surface plasmon coupled emission[23] occurs when an emitter lies at the truncation interface of a proper 1DPC with its dipole moment lying on the surface.[24] In this case, the emitted energy couples to BSW and propagates parallel to the 1DPC surface, with specific momentum and polarization according to the BSW mode dispersion.[25] In this respect, BSW on 1DPC has a role similar to propagating plasmons on metallic films without the drawback of ohmic absorption. In addition, the 1DPC can be designed to sustain BSWs in the desired spectral region and with the desired polarization, not necessarily restricted to the TE case.

In recently published works, an off-axis beam has been obtained by diffracting surface plasmons locally coupled through the use of nanoslits with a pair of linear gratings having different periods.[19,26] In order to check the validity of this approach on a BSW-based system, we built up a two-dimensional computational model consisting of a pair of additive linear gratings located on a 1DPC as defined above. Gratings can be made of any low-absorbing dielectric material, including polymers. At a height of 5 nm over a flat area between the two gratings, an emitting source is introduced in the form of a line of current (Figure 2a). The line of current is oriented along the y-axis and emits a TE-polarized radiation that can couple to BSWs. The emitted spectrum ranges from 550 to 600

dx.doi.org/10.1021/ph500095y | ACS Photonics 2014, 1, 612−617

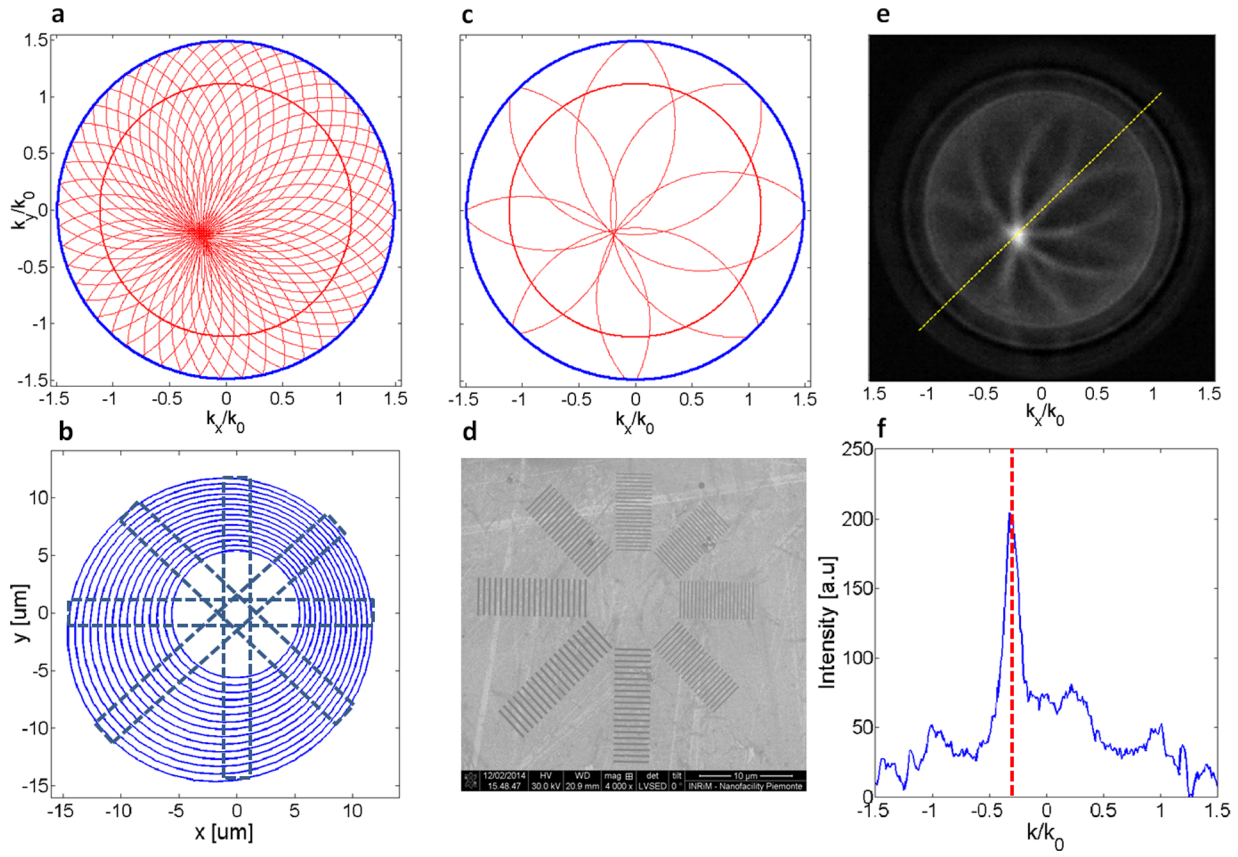

Figure 3. (a) Calculated diffraction pattern in the Fourier plane produced by a circular grating described by $\vec{G}(\varphi) = G_0(1 - 0.28\sin(\varphi + \pi/4))\cdot\vec{u}_r$, where $G_0 = \beta_{BSW}$ and φ is considered counterclockwise from the x-axis. The outer blue circle indicates the maximum NA of observation, while the inner red, thick circle is the BSW ring at λ = 570 nm. (b) Ideal anisotropic circular grating associated with the pattern in (a). The dashed boxes indicate the region of discretization for the real structure. (c) BSW diffraction pattern in the Fourier plane produced by a subset of eight linear gratings extracted from (b). (d) SEM image of a real grating obtained from the discretization in (b). (e) Measured back focal plane showing diffracted BSW-assisted fluorescence. (f) Fluorescence intensity profile cross-section along the yellow dashed line in (e).

nm in wavelength. Details about the model can be found in the Methods section. The period of the gratings is chosen in such a way that diffracted BSWs in the glass substrate superpose at an angle $\theta_{beam} = 10°$ with respect to the normal surface. In a first approximation, this effect can be described by applying the diffraction Bragg's law (at the first-order) for the two gratings, as described by the following equations:

$$G_1 = \beta_{BSW} - k_0 n_s \sin(\theta_{beam}) \quad (1)$$

$$G_2 = \beta_{BSW} + k_0 n_s \sin(\theta_{beam}) \quad (2)$$

where $G_{1,2} = 2\pi/\Lambda_{1,2}$ are the grating vectors for the two gratings with periods Λ_1 and Λ_2, respectively, β_{BSW} is the BSW wavevector component parallel to the 1DPC surface, n_s is the refractive index of the glass substrate, and $k_0 = 2\pi\lambda^{-1}$ is the wavenumber of the radiation emitted in vacuum at a given wavelength λ. As an example, by setting $\theta_{beam} = 10°$, the periods Λ_1 and Λ_2 can be calculated from eqs 1 and 2 for a specific wavelength. However, the presence of a grating itself produces a slight increase of β_{BSW} as compared to the case of a bare 1DPC surface, depending on the grating height (because of a dielectric-loading red-shift[27]), and an iterative optimization should be performed in order to find the most suitable grating parameters by taking into account the effective β_{BSW}.

We optimized the beaming effect for λ = 570 nm, resulting in grating periods Λ_1 = 670 nm and Λ_2 = 415 nm. Provided that such a model works in a single direction only, it is indeed possible to observe a BSW-mediated diffraction similar to the plasmonic case. Figure 2b show the calculated near-field intensity distribution of the electromagnetic field emitted by the source. It is worth underlining how the coupling of the electromagnetic field to BSW can be easily appreciated close to the emitter. The BSW-coupled radiation propagates along the surface and gets diffracted by the two gratings. On a wider spatial scale (Figure 2c), the combined diffraction by the grating pair results in two tilted beams propagating in air and in glass, respectively, with the last one having a suitable propagation angle. When the far-field intensity angular pattern is considered (see Methods section), a clear beaming of the power radiated by the source can be observed, with very low divergence; $\Delta\theta_{beam} \approx 1.1°$ in glass and $\Delta\theta_{beam} \approx 1.7°$ in air (Figure 2d). The two beams propagating in air and in glass bring 33% and 12% of the total power emitted by the source, respectively. In particular, considering only the emission within the glass substrate, the BSW-assisted beam corresponds to 67% of the emitted power.

When extending the working principle above-described to a three-dimensional scenario, a circularly symmetric diffractive structure can be considered. In a previous work, we experimentally demonstrated that BSW-coupled fluorescence can be efficiently beamed by means of surface corrugations periodically arranged around the feeding source.[21] However,

dx.doi.org/10.1021/ph500095y | ACS Photonics 2014, 1, 612−617

the tilting of the BSW-assisted beam requires some loss of symmetry in the diffractive structure.[18] Here we propose an anisotropic circular grating with a spatially varying periodicity. More specifically, we consider a diffractive circular structure with a grating period that is varying azimuthally. Such a grating can be obtained from a local application of the Bragg law to a corresponding diffraction pattern defined over the Fourier plane.

In a Fourier plane defined by the axis k_x/k_0 and k_y/k_0, where k_x and k_y are the x- and y-components of the transverse wavevector parallel to the 1DPC surface, we consider a circular region within the light line in glass, i.e., $((k_x/k_0)^2 + (k_y/k_0)^2)^{1/2} \leq 1.49$ (outer blue line in Figure 3a).

This portion of the Fourier plane represents the angular range of collection in an eventual microscope-based system and can be directly imaged in a leakage radiation setup with back focal plane imaging capabilities (e.g., by using an oil immersion objective with numerical aperture (NA) = 1.49).[28]

At a specific wavelength, the BSW on the planar 1DPC can be represented on the Fourier plane as a ring having radius[29]

$$\sqrt{(k_x/k_0)^2 + (k_y/k_0)^2} = \beta_{BSW}(\lambda)/k_0$$

When a grating is added onto the 1DPC surface, the BSW gets diffracted accordingly. In the Fourier plane, a replica of the BSW ring is produced as shifted from its central position $k_x/k_0 = k_y/k_0 = 0$ by a length proportional to the grating vector.[30] The direction of such a displacement is parallel to the grating vector. In the case of a circular grating with a spatial period varying with the azimuthal angle φ, a resulting grating $G(\varphi)\cdot\vec{u}_r$ is obtained, where $\vec{u}_r$ is the unitary radial vector in the Fourier plane. Therefore, a plurality of diffracted BSW rings will be obtained by radially shifting the BSW ring by a length $G(\varphi)$ as multiple azimuthal directions from $\varphi = 0$ to $\varphi = 2\pi$ are considered.

The function $G(\varphi)$ can be designed in such a way that most of the diffracted BSW rings superpose each other over a small region in the Fourier plane, eventually not centered at $k_x/k_0 = k_y/k_0 = 0$, thus leading to a beaming effect. In the following, we apply this mechanism to a specific case, whose results are summarized in Figure 3. As for linear gratings, however, the effective β_{BSW} of a BSW subjected to diffraction is slightly increased as compared to the BSW on a bare 1DPC because of a dielectric loading effect caused by the additional layer including the grating.

We consider a $\lambda = 570$ nm BSW propagating on a 1DPC coated with a polymeric additional layer 40 nm thick. The corresponding BSW wavevector is calculated as $\beta_{BSW}/k_0 \cong 1.115$, and it is represented by the thick red circle in Figure 3a. The thickness of the polymeric layer used for estimating β_{BSW}/k_0 is chosen to be one-half the thickness of the final grating that will be fabricated on the 1DPC (because the grating has a fill factor of 0.5).

An anisotropic circular grating defined by

$$\vec{G}(\varphi) = G_0(1 - 0.28\sin(\varphi + \pi/4))\cdot\vec{u}_r$$

diffracts BSW in such a way that most of the diffracted first-orders superpose in a small region at $\beta_{beam}/k_0 = 0.3$, where β_{beam} is the transverse wavevector component of the out-coupled radiation beamed. The beaming angle corresponds to an angular tilt of about 11.5° with respect to the surface normal, in the glass substrate. The grating structure producing the diffraction pattern in Figure 3a can be obtained by sequentially applying the Bragg law on a set of local linear gratings radially oriented, each of them associated with a specific azimuthal angle φ.

The result is shown in Figure 3b, wherein the corrugations surround a wide flat central area with a diameter of 10 μm. The grating structure depicted in Figure 3b may be difficult to fabricate. Therefore, we reduced the complexity by discretizing the circular structure along four specific directions, namely, horizontal, vertical, and two diagonals tilted at 45° (as indicated by the dashed boxes in Figure 3b). In addition, the corresponding diffraction branches are further optimized in such a way that they are intersecting onto a single point in the Fourier space (Figure 3c). As a result, eight gratings oriented along the four directions defined above are obtained.

Fabrication is performed by electron beam lithography (EBL), using a negative tone resist with a thickness of about 80 nm (details in the Methods section). The final structure is shown in the scanning electron microscope (SEM) image in Figure 3d.

In order to investigate the coupling of localized light emitters with the photonic structure, the 1DPC has been coated with a uniform thin fluorescent layer of protein A labeled with AlexaFluor546. The emission spectrum of AlexaFluor 546 is shown as superposed to the 1DPC reflectivity map in Figure 1a. It can be appreciated that the maximum of emission corresponds to a wavelength $\lambda = 570$ nm.

A customized setup is used to collect fluorescence and image the back focal plane (BFP) of the collecting objective. Fluorescence is excited in the very center of the structure by means of a Nd:YAG laser beam ($\lambda = 532$ nm) coming from the air side and focused by an objective (Zeiss Ultrafluar 10×, NA = 0.2). Fluorescence is collected from the glass substrate side by means of an oil immersion objective with high numerical aperture (Nikon APO TIRF 100×, NA = 1.49). After filtering out the laser radiation with an edge filter (RazorEdge Longpass 532), the BFP is imaged onto a CMOS camera (Thorlabs DCC1645C) via a tube lens. The experimental result is shown in Figure 3e and can be directly compared to Figure 3c as expected from our model calculation. We indeed observe that all the diffracted branches superpose in the bright point out of the center of the BFP, meaning that an effective beaming effect has been obtained off-normal. An intensity profile (Figure 3f) plotted along the yellow dashed line in Figure 3d exhibits a main peak centered at $\beta_{beam}/k_0 = 0.3$, corresponding to the suitable output angle of about 11.5° in glass. The width of the beam is larger than expected because of the broadband emission of the fluorescent dye. In fact, the grating has been optimized for $\lambda = 570$ nm, while AlexaFluor 546 has an emission spectrum ranging from 550 to 620 nm in wavelength. However, despite the broad spectrum of fluorescence involved, the beaming effect still shows a rather low angular divergence, estimated as $\Delta\theta_{beam} \approx 8°$ (full width at half-maximum of the BFP peak) from the BFP image.

In conclusion we have demonstrated that the radiation emitted by localized sources can be angularly beamed in a three-dimensional collimated off-axis beam. Such a result is obtained by employing a fully dielectric structure mimicking a plasmonic substrate wherein the surface energy carriers are represented by BSWs instead of surface plasmons. The main advantages of the proposed arrangement are connected to the use of all-dielectric materials, whereby losses are dramatically reduced. In addition, it is possible to design this kind of structure for operating as desired in a very large spectral range,

dx.doi.org/10.1021/ph500095y | ACS Photonics 2014, 1, 612−617

from UV to NIR.[31,32] The additive diffractive structures can be fabricated with polymeric materials. Taking advantage of their electromechanical properties yielding suitable actuation strain, active dynamic control of the radiation pattern could be achieved.[15]

METHODS

Sample. The 1DPC consists of a periodic stack of dielectric thin films made of Ta_2O_5 (high refractive index) and SiO_2 (low refractive index) layers, deposited on a glass coverslip 150 μm thick by plasma-ion-assisted deposition under high-vacuum conditions (APS904 coating system, Leybold Optics). The stack sequence is glass−$[Ta_2O_5-SiO_2]\times10-Ta_2O_5-SiO_2$−air, with 22 layers in total. The Ta_2O_5 layer is 95 nm thick, the SiO_2 layer is 137 nm thick, but the very last SiO_2 layer on top of the stack is only 127 nm thick.

The gratings have been fabricated by electron beam lithography on a negative tone resist (Ma-N 2401 from microResist Technology). The resist has been spin coated on the 1DPC at 4000 rpm for 30 s in order to have a 80 nm thick layer. The EBL process has been performed under low-vacuum condition (chamber pressure 40 Pa) to prevent charging effects, since the lithography is directly performed on an insulating substrate. The sample has been developed in ma-D 332 for 30 s and then rinsed in water.

In order to make the photonic structure fluorescent, 60 μL of PtA conjugated with AlexaFluor 546 diluted in water (1 μg/mL) has been incubated for 20 min on the sample surface. The sample has then been rinsed with PBS to remove the excess PtA not adsorbed onto the surface.

Computational Model. The 2D model has been implemented in the COMSOL 4.2a RF module using the frequency domain solver. The spatial domain is surrounded by perfectly matched layers . The emitting source is modeled with an out-of-plane line of current that ensures a TE polarization of the emitted radiation.

The far-field radiation pattern in Figure 2d has been calculated by postprocessing the near-field distribution of the electromagnetic field, with a tool provided in COMSOL based on the surface equivalent theorem.

AUTHOR INFORMATION

Corresponding Authors

*E-mail: angelo.angelini@polito.it. Phone: +39 011-0907343.
*E-mail: emiliano.descrovi@polito.it. Phone: +39 011-0907354.

Notes

The authors declare no competing financial interest.

ACKNOWLEDGMENTS

This research has received funding from the Italian Flagship Project NANOMAX (Progetto Bandiera MIUR PNR 2011−2013) and the EU FP7 project BILOBA (Grant No. 318035). EBL fabrication has been performed at Nanofacility Piemonte INRIM, a laboratory supported by Compagnia di San Paolo Foundation.

REFERENCES

(1) Novotny, L.; Van Hulst, N. Antennas for light. *Nat. Photonics* **2011**, *5*, 83−90.
(2) Noda, S.; Fujita, M.; Asano, T. Spontaneuos emission control by photonic crystals and nanocavities. *Nat. Photonics* **2007**, *1*, 449−458.
(3) Lee, G. K.; Chen, X. W.; Eghlidi, H.; Kukura, P.; Lettow, R.; Renn, A.; Sandoghdar, V.; Gotzinger, S. A planar dielectric antenna for directional single-photon emission and near-unity collection efficiency. *Nat. Photonics* **2011**, *5*, 166−169.
(4) Ganesh, N.; Zhang, W.; Mathias, P. C.; Chow, E.; Soares, J. A. N. T.; Malyarchuk, V.; Smith, A. D.; Cunningham, B. T. Enhanced fluorescence emission from quantum dots on a photonic crystal surface. *Nat. Nanotechnol.* **2007**, *2*, 315−320.
(5) Fehrembach, A. L.; Enoch, S.; Sentenac, A. Highly directive light sources using two-dimensional photonic crystal slabs. *Appl. Phys. Lett.* **2001**, *79*, 4280.
(6) Kramper, P.; Agio, M.; Soukoulis, C. M.; Birner, A.; Müller, F.; Wehrspohn, R. B.; Gösele, U.; Sandoghdar, V. Highly directional emission from photonic crystal waveguides of subwavelength width. *Phys. Rev. Lett.* **2004**, *92*, 113903.
(7) Moreno, E.; Garcìa-Vidal, F. J.; Martin-Moreno, L. Enhanced transmission and beaming of light via photonic crystal surface modes. *Phys. Rev. B* **2004**, *69*, 121402(R).
(8) Taminiau, T. H.; Stefani, F. D.; Segerink, F. B.; Van Hulst, N. Optical antennas direct single molecule emission. *Nat. Photonics* **2008**, *2*, 234−237.
(9) Curto, A. G.; Volpe, G.; Taminiau, T. H.; Kreuzer, M. P.; Quidant, R.; Van Hulst, N. Unidirectional emission of a quantum dot coupled to a nanoantenna. *Science* **2010**, *329*, 930−933.
(10) Kosako, T.; Kadoya, Y.; Hofmann, H. F. Directional control of light by a nano-optical Yagi-Uda antenna. *Nat. Photonics* **2010**, *4*, 312−315.
(11) Filter, R.; Qi, J.; Rockstuhl, C.; Lederer, F. Circular optical nanoantennas: an analytical theory. *Phys. Rev. B* **2012**, *85*, 125429.
(12) Kern, A. M.; Martin, O. J. F. Excitation and emission of molecules near realistic plasmonic nanostructures. *Nano Lett.* **2011**, *11* (2), 482−487.
(13) Lozano, G.; Louwers, D. J.; Rodriguez, S. R. K; Murai, S.; Jansen, O. T. A.; Verschuuren, M. A.; Gomez-Rivas, J. Plasmonics for solid-state lighting: enhanced excitation and directional emission of highly efficient light sources. *Light: Sci. Appl.* **2013**, *2*, e66.
(14) Langguth, L.; Punj, D.; Wenger, J.; Koenderink, A. F. Plasmonic band structure controls single-molecule fluorescence. *ACS Nano* **2013**, *7*, 8840−8848.
(15) Li, H.; Xu, S.; Gu, Y.; Wang, H.; Ma, R.; Lombardi, J. R.; Xu, W. Active plasmonic nanoantennas for controlling fluorescence beams. *J. Phys. Chem. C* **2013**, *117*, 19154−19159.
(16) Choy, J. T.; Bulu, I.; Hausmann, B. J. M.; Janitz, E.; Huang, I. C.; Loncar, M. Spontaneous emission and collection efficiency enhancement of single emitters in diamond via plasmonic cavities and gratings. *Appl. Phys. Lett.* **2013**, *103*, 161101.
(17) Ebbesen, T. W.; Lezec, H. J.; Ghaemi, H. F.; Thio, T.; Wolff, P. A. Extraordinary optical transmission through sub-wavelength hole arrays. *Nature* **1998**, *391*, 667−669.
(18) Lezec, H. J.; Degiron, A.; Deveaux, E.; Linke, R. A.; Martin-Moreno, L.; Garcia-Vidal, F. J.; Ebbesen, T. W. Beaming light from a subwavelength aperture. *Science* **2002**, *297*, 820−822.
(19) Jun, C. Y.; Huang, K. C. Y.; Brongersma, M. L. Plasmonic beaming and active control over fluorescent emission. *Nat. Commun.* **2011**, *2*, 283.
(20) Aouani, H.; Mahboub, O.; Devaux, E.; Rigneault, H.; Ebbesen, T. W.; Wenger, J. Plasmonic antennas for directional sorting of fluorescence emission. *Nano Lett.* **2011**, *11*, 2400−2406.
(21) Angelini, A.; Barakat, E.; Munzert, P.; Boarino, L.; De Leo, N.; Enrico, E.; Giorgis, F.; Herzig, H. P.; Pirri, C. F.; Descrovi, E. Focusing and extraction of light mediated by Bloch surface waves. *Sci. Rep.* **2014**, *4*, 5428.
(22) Rui, G.; Abeysinghe, D. C.; Nelson, L. R.; Zhan, Q. Demonstration of beam steering via dipole-coupled plasmonic spiral antenna. *Sci. Rep.* **2013**, *3*, 2237.
(23) Lakowicz, J. R.; Ray, K.; Chowdhury, M.; Szmacinski, H.; Fu, Y.; Zhang, J.; Nowaczyk, K. Plasmon controlled fluorescence: a new paradigm in fluorescence spectroscopy. *Analyst* **2008**, *133*, 1308−1346.

(24) Badugu, R.; Nowazcyk, K.; Descrovi, E.; Lakowicz, J. R. Radiative decay engineering 6: Fluorescence on one-dimensional photonic crystals. *Anal. Biochem.* **2013**, *442*, 83−96.
(25) Ballarini, M.; Frascella, F.; Enrico, E.; Mandracci, P.; De Leo, N.; Michelotti, F.; Giorgis, F.; Descrovi, E. Bloch surface waves-controlled fluorescence emission: coupling into nanometer-sized polymeric waveguides. *Appl. Phys. Lett.* **2012**, *100*, 063305.
(26) Kim, S.; Kim, H.; Lim, Y.; Lee, B. Off-axis directional beaming of optical field diffracted by a single subwavelength metal slit with asymmetric dielectric surface gratings. *Appl. Phys. Lett.* **2007**, *90*, 051113.
(27) Ballarini, M.; Frascella, F.; De Leo, N.; Ricciardi, S.; Rivolo, P.; Mandracci, P.; Enrico, E.; Giorgis, F.; Michelotti, F.; Descrovi, E. A polymer-based functional pattern on onedimensional photonic crystals for photon sorting of fluorescence radiation. *Opt. Express* **2012**, *20*, 6703−6711.
(28) Drezet, A.; Hoheanu, A.; Koller, D.; Stepanov, A.; Ditlbacher, H.; Steinberger, B.; Ausseneg, F. R.; Leitner, A.; Krenn, J. R. Leakage radiation microscopy of surface plasmon polaritons. *Mater. Sci. Eng., B* **2008**, *14*, 220−229.
(29) Angelini, A.; Enrico, E.; De Leo, N.; Munzert, P.; Boarino, L.; Michelotti, F.; Giorgis, F.; Descrovi, E. Fluorescence diffraction assisted by Bloch surface waves on a one-dimensional photonic crystal. *New J. Phys.* **2013**, *15*, 073002.
(30) Lopez-Boada, R.; Regan, C.; Dominguez, D.; Bernussi, A.; Grave de Peralta, L. Fundaments of optical far-field subwavelength resolution based on illumination with surface waves. *Opt. Express* **2013**, *21*, 11928−11942.
(31) Farmer, A.; Friedli, C. A.; Wright, S. M.; Robertson, W. M. Biosensing using surface electromagnetic waves in photonic bandgap multilayers. *Sens. Actuators B* **2012**, *173*, 79−84.
(32) Descrovi, E.; Sfez, T.; Quaglio, M.; Brunazzo, D.; Dominici, L.; Michelotti, F.; Herzig, H. P.; Martin, O. J. F.; Giorgis, F. Guided Bloch surface waves on ultrathin polymeric ridges. *Nano Lett.* **2010**, *10*, 2087−2091.